Wigner crystal thermoelectricity, diode and quantum computing

Dima Shepelyansky
www.quantware.ups-tlse.fr/dima

with D.Demidov (RAS Kazan), J.Lages (UTINAM Besancon), M.Zakharov (U Kazan), O.Zhirov (BINP Novosibirsk)

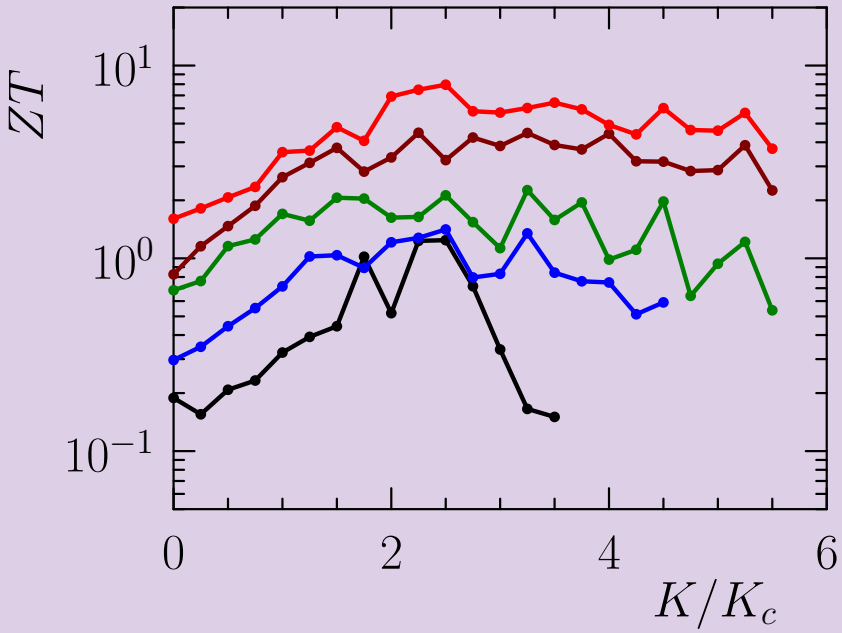

- Frenkel-Kontorova model and Wigner crystal in a periodic potential; Chirikov standard map; Aubry pinned phase
- Thermoelectricity with high figure of merit ($ZT \approx 8$)
- Diode charge transport in asymmentric periodic potential
- Quantum computer with electrons on a liquid helium in the Aubry pinned phase?

Support: LABEX NEXT THETRACOM project (disruptive)

Thermoelectricity at nanoscale: theoretical models

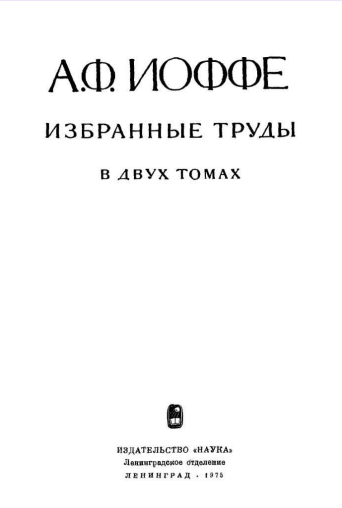

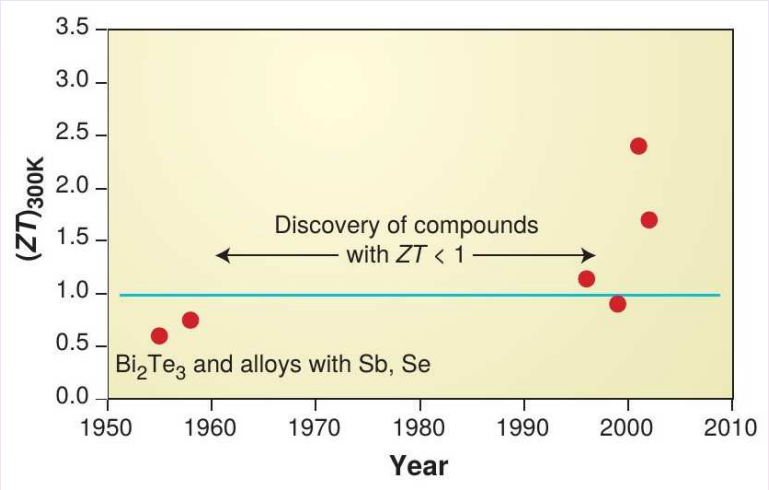

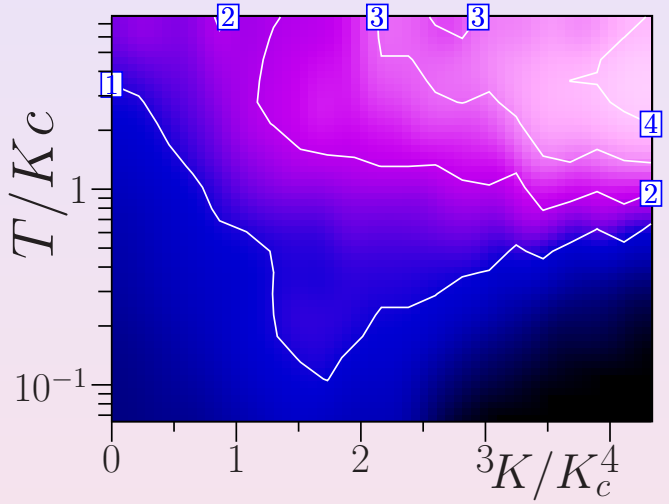

Left: A.F.Ioffe book (1956)
Center: figure of merit *ZT* with time (A.Majumdar Science **303**, 777 (2004))
Right panel: ZT diagram (Zhirov, DS EPL **103**, 68008 (2013))

Early works

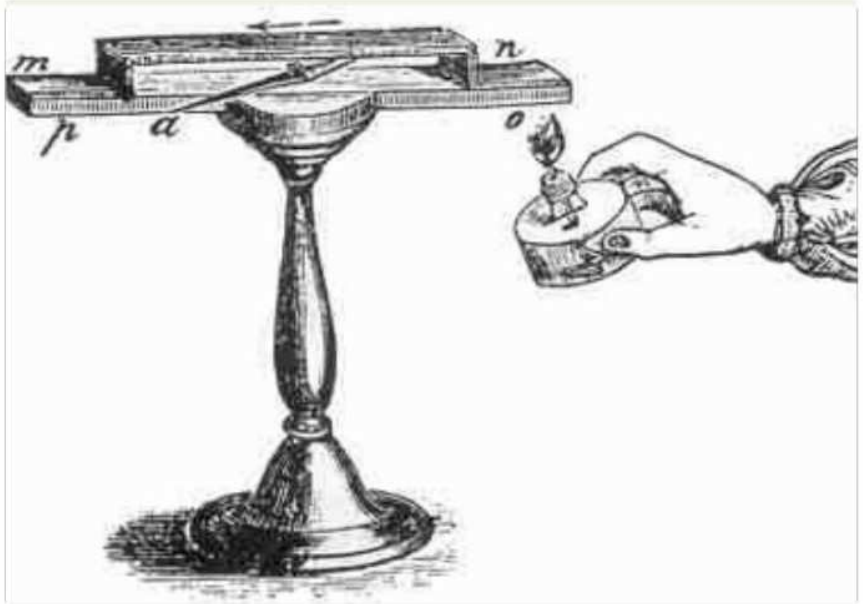

T. Seebeck-deflection of a compass needle (circa 1823)

from Y.Imry (Weizmann Inst) talk at Inst. H. Poincaré, Paris (2012)

Early works

A. F. Ioffe

semiconductors

and figure of merit

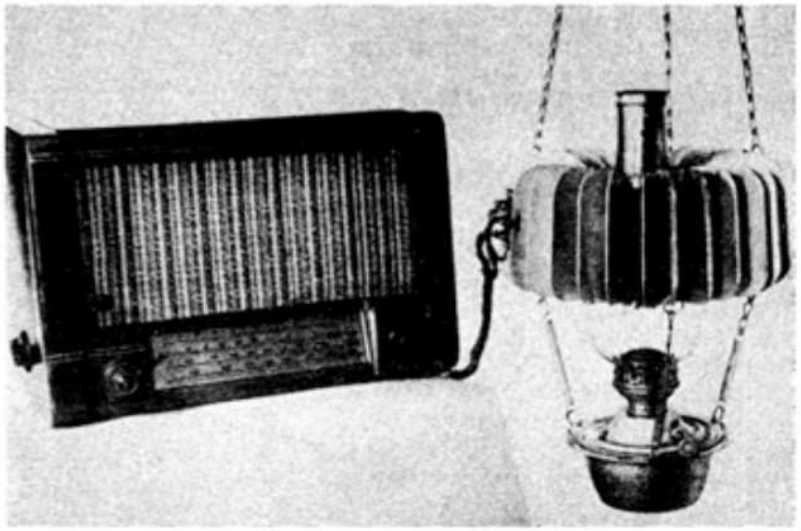

Oil burning lamp powering a radio using the first commercial thermoelectric generator containing ZnSb built in USSR, circa 1948

from Y.Imry (Weizmann Inst) talk at Inst. H. Poincaré, Paris (2012)

Main characteristics

Seebeck coefficient:

$S = \Delta V/\Delta T = \pi^2 {k_B}^2 T[(d\ln\sigma/dE)]|_{E_F}/e$ (Mott relation (1958))

For 2DEG with Wiedemann-Franz law: $S = 2\pi {k_B}^2 Tm/(3eh^2 n_e)$;

typical value $S \approx 10\mu V/K$ at $T = 0.3K$, $n_e = 4 \cdot 10^{10} cm^{-2}$

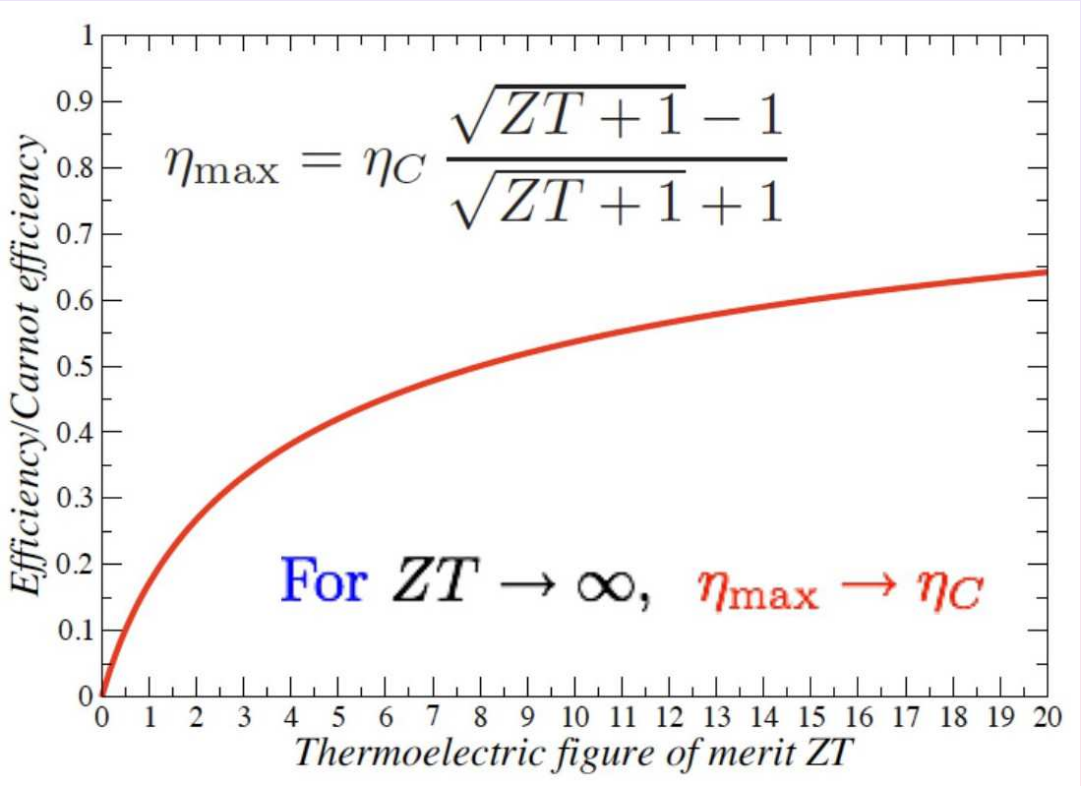

Thermoelectric figure of merit $ZT = \sigma S^2 T/\kappa$,

thermoefficiency $\eta_{max} = \eta_{Carnot}(\sqrt{ZT+1}-1)/(\sqrt{ZT+1}+1)$

thermal conductivity $\kappa = \kappa_{el} + \kappa_{phonon}$ (heat flux $Q = -\kappa \nabla T$)

Experiments on Seebeck coefficient for 2DEG

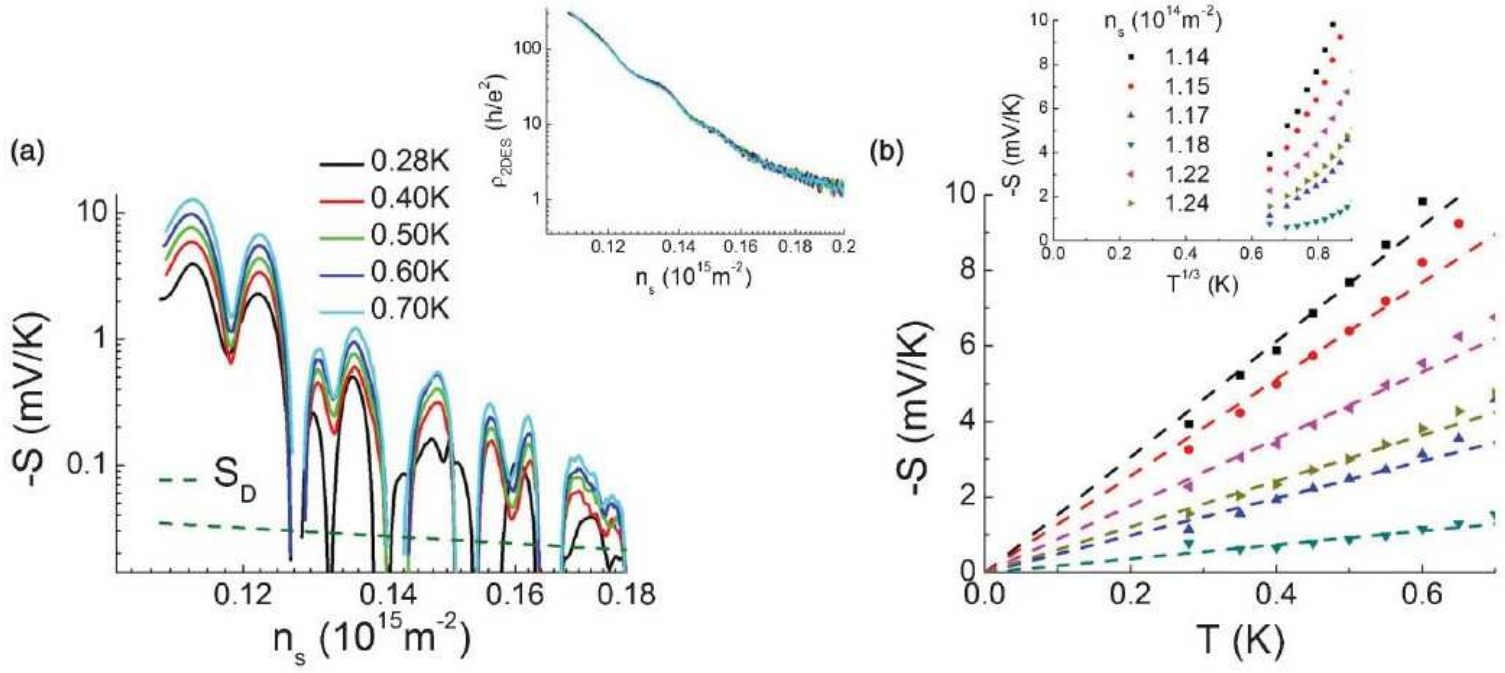

FIG. 5. (Color online) (a) S vs n_s for 0.28 K $< T <$ 0.7 K. The broken green line shows S_d [Eq. (2)] at 0.28 K. Inset: ρ_{2DES} vs n_s at the same T values; there is little T dependence in this range. (b) Low-T linear variation of S. Inset: Descriptions based on variable-ranged hopping, where S is expected to decay to zero as $T^{1/3}$, do not adequately describe the observed data.

V.Narayan, S.Goswami, M.Pepper et al. PRB **85**, 125406 (2012)

In dimensionless units $S = 10mV/K \approx 100 \gg 1$ $(e = k_B = 1)$

ZT in *SnSe*

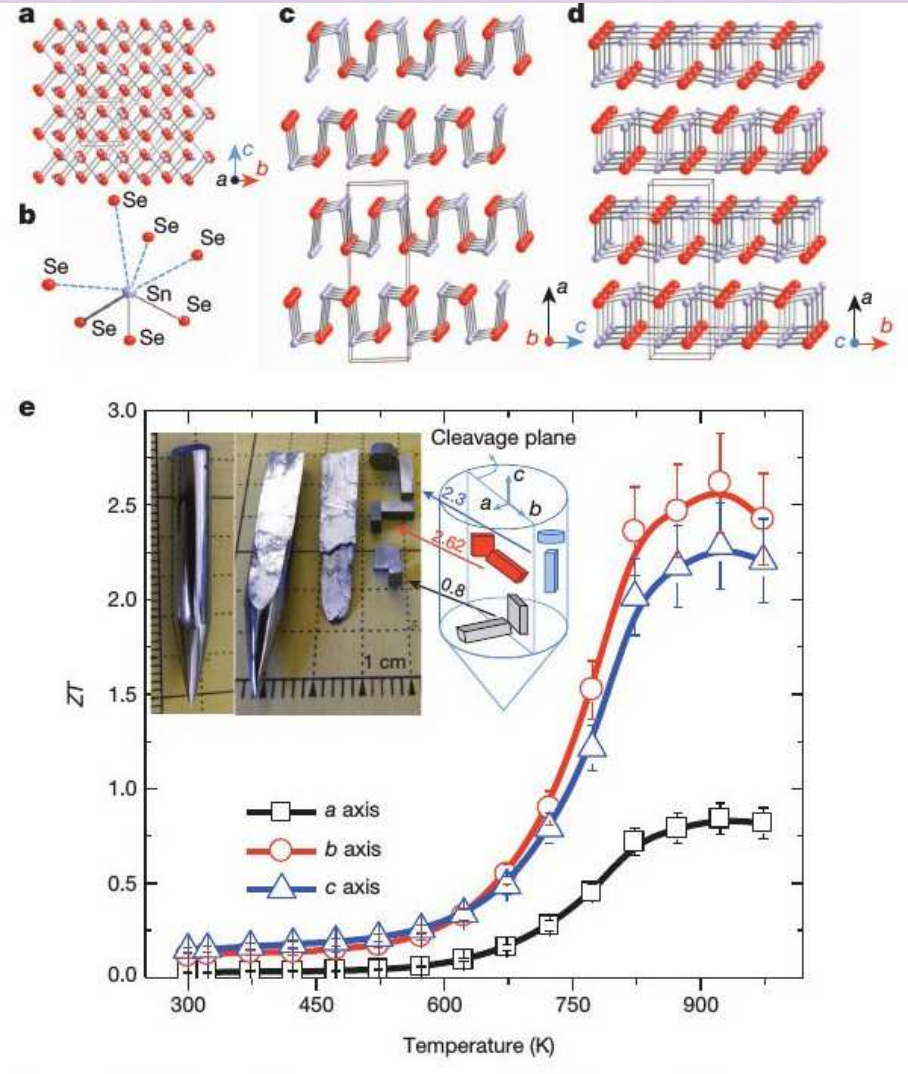

Figure 1 | SnSe crystal structure *Pnma* and *ZT* values. **a**, Crystal structure along the *a* axis: grey, Sn atoms; red, Se atoms. **b**, Highly distorted $SnSe_7$ coordination polyhedron with three short and four long Sn–Se bonds. **c**, Structure along the *b* axis. **d**, Structure along the *c* axis. **e**, Main panel, *ZT* values along different axial directions; the *ZT* measurement uncertainty is about 15% (error bars). Inset images: left, a typical crystal; right, a crystal cleaved along the (l00) plane, and specimens cut along the three axes and corresponding measurement directions. Inset diagram, how crystals were cut for directional measurements; *ZT* values are shown on the blue, red and grey arrows; colours represent specimens oriented in different directions.

Li-Dong Zhao et al. (Illinois) Nature **508**, 373 (2014)

maximal $ZT \approx 2.6$ in materials

Frenkel-Kontorova model (ZhETF 1938)

Chirikov standard map (1969-1979); Aubry transition $K > K_c = 0.9716$ (1983)

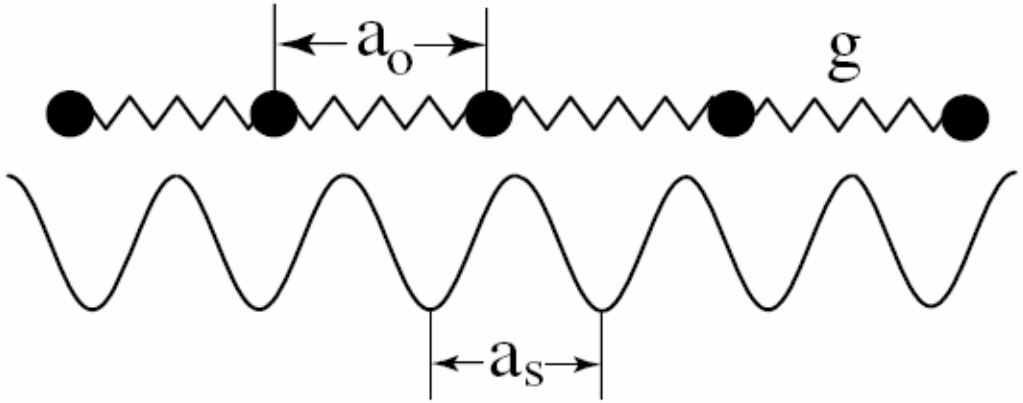

Fig. 1.1. Schematic presentation of the Frenkel-Kontorova model: A chain of particles interacting via harmonic springs with elastic coupling g is subjected to the action of an external periodic potential with period a_s.

Introducing the dimensionless variables, we re-write the Hamiltonian (1.1)–(1.5) in the conventional form ($H = 2\mathcal{H}/\varepsilon_s$)

$$H = \sum_n \left\{ \frac{1}{2}\left(\frac{dx_n}{dt}\right)^2 + (1 - \cos x_n) + \frac{g}{2}(x_{n+1} - x_n - a_0)^2 \right\}, \qquad (1.8)$$

fixed particle density $\nu = 0.618...$ $\rightarrow$ golden KAM curve

O.M.Braun and Yu.S.Kivshar, *The Frenkel-Kontorova model ...* Spriner (2004)

Wigner crystal in a periodic potential

The dimensionless Hamiltonian has the form:

$$H = \sum_{i=1}^{N} (\frac{P_i^2}{2} - K \cos x_i) + \sum_{i>j} \frac{1}{|x_i - x_j|} \quad (1)$$

where P_i, x_i are ion momentum and position, K gives the strength of optical lattice potential and all N ions are placed in a harmonic potential with frequency ω. To make a transfer from (1) to dimensional physical units one should note that the lattice constant d in $K \cos(x_i/d)$ is taken to be unity, the energy $E = H$ is measured in units of ion charge energy e^2/d. In the quantum case $P_i = -i\hbar\partial/\partial x_i$ with dimensionless $\hbar$ measured in units $\hbar \to \hbar/(e\sqrt{md})$, m is charge mass.

Related map:

$$p_{i+1} = p_i + Kg(x_i) \ , \quad x_{i+1} = x_i + 1/\sqrt{p_{i+1}} \ , \quad (2)$$

where the effective momentum conjugated to x_i is $p_i = 1/(x_i - x_{i-1})^2$ and the kick function is $Kg(x) = -K \sin x$.

For the Frenkel-Kontorova model the equilibrium positions are described by the Chirikov standard map (1969-1979): $p_{i+1} = p_i + K \sin x_i, \ x_{i+1} = x_i + p_{i+1}$ with $K_c = 0.971635...$ for the golden mean density $\nu = (\sqrt{5} + 1)/2$.

I.Garcia-Mata, O.V.Zhirov, D.S. EPJD **41**, 325 (2007) $\to K_c = 0.046$ *vs.* 0.034

Classical Wigner crystal: map, spectrum

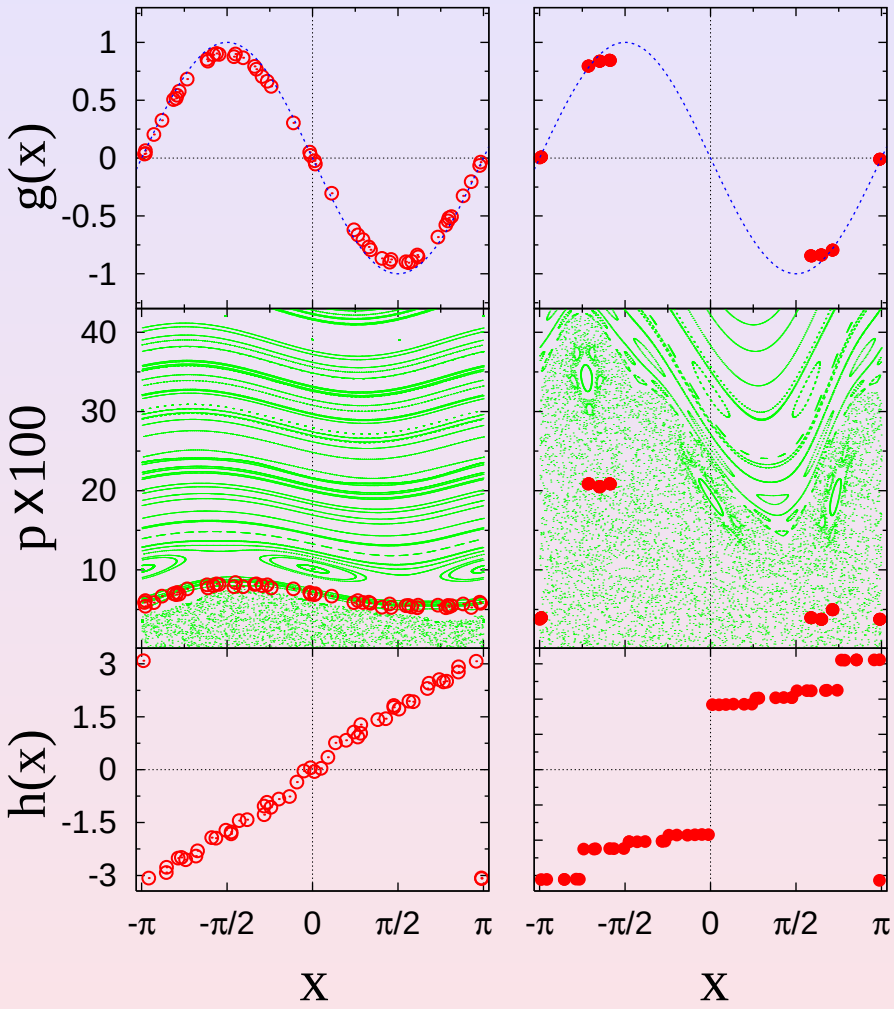

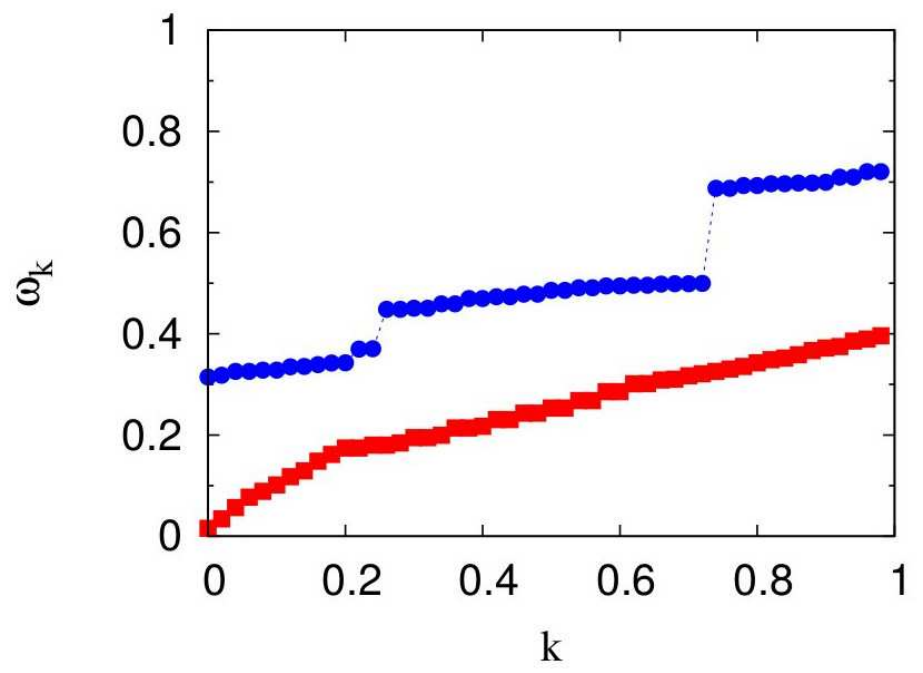

$N = 150$ ions in oscillator potential (central part) at $K = 0.03$ (left/red), $K = 0.2$ (right/blue); $\nu \approx 1.618$

Density dependence of Aubry transition

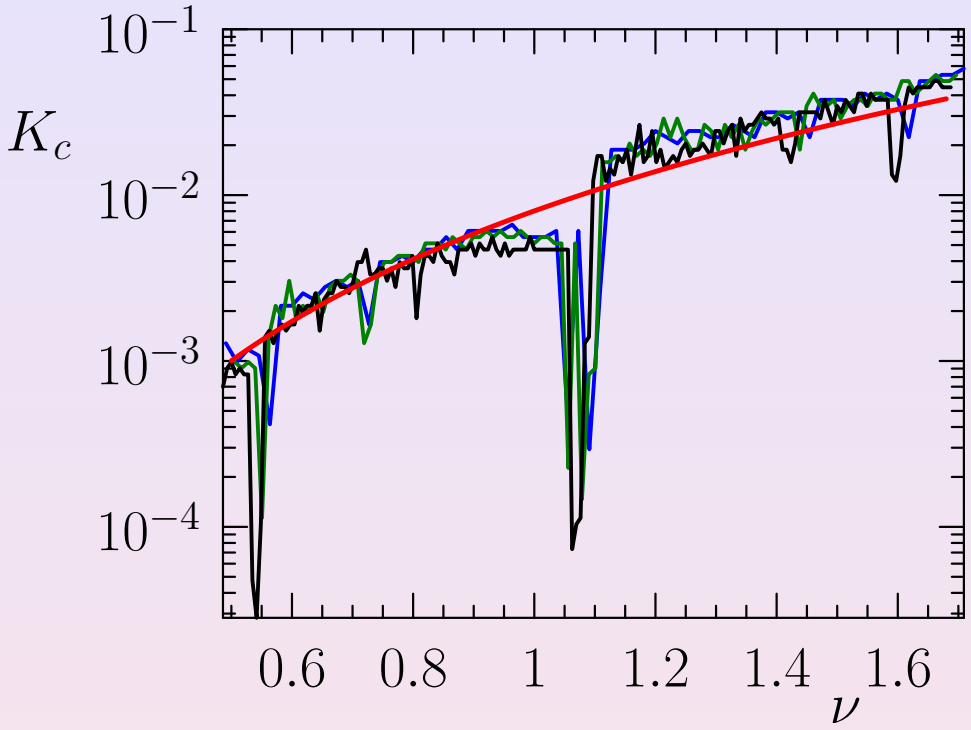

Linearized approximation by the Chirikov standard map gives
$K_c = 0.034(\nu/1.618)^3$
Numerical data for number of wells $L = 55, 89, 144$ and varied number of electrons/ions N with $\nu = N/L$;
red curve is from the Chirikov standard map approximation
Zhirov, Lages, DS (EPJD 2019 in print)

Dynamical spin-glass in Aubry pinned phase

Quantum Monte Carlo computations

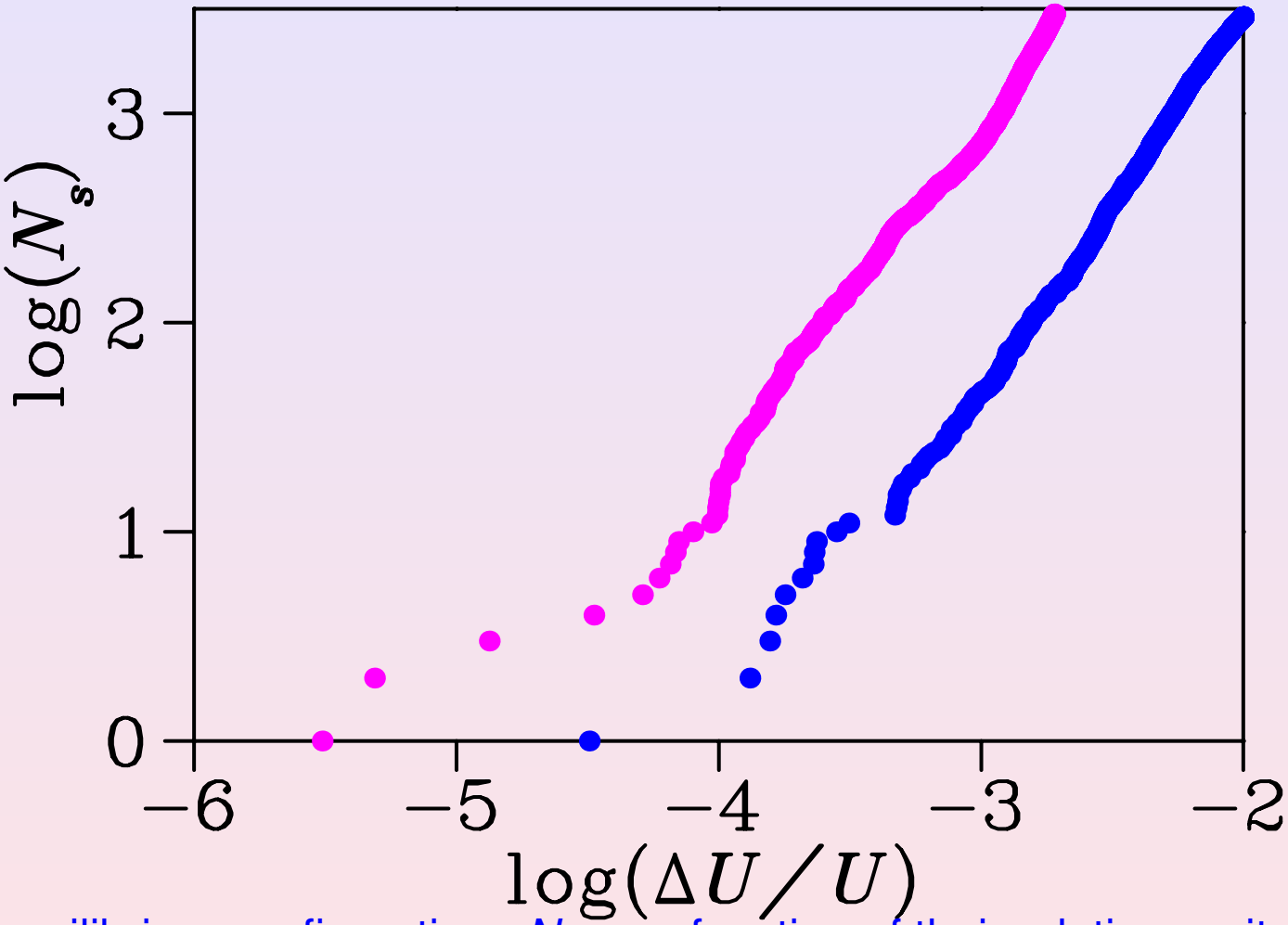

Number of equilibrium configurations N_s as a function of their relative excitation energy $\Delta U/U$ above the ground state for 50 (blue) and 150 (magenta) ions at $K = 0.2$ (logarithms are decimal).

Quantum melting of Wigner crystal

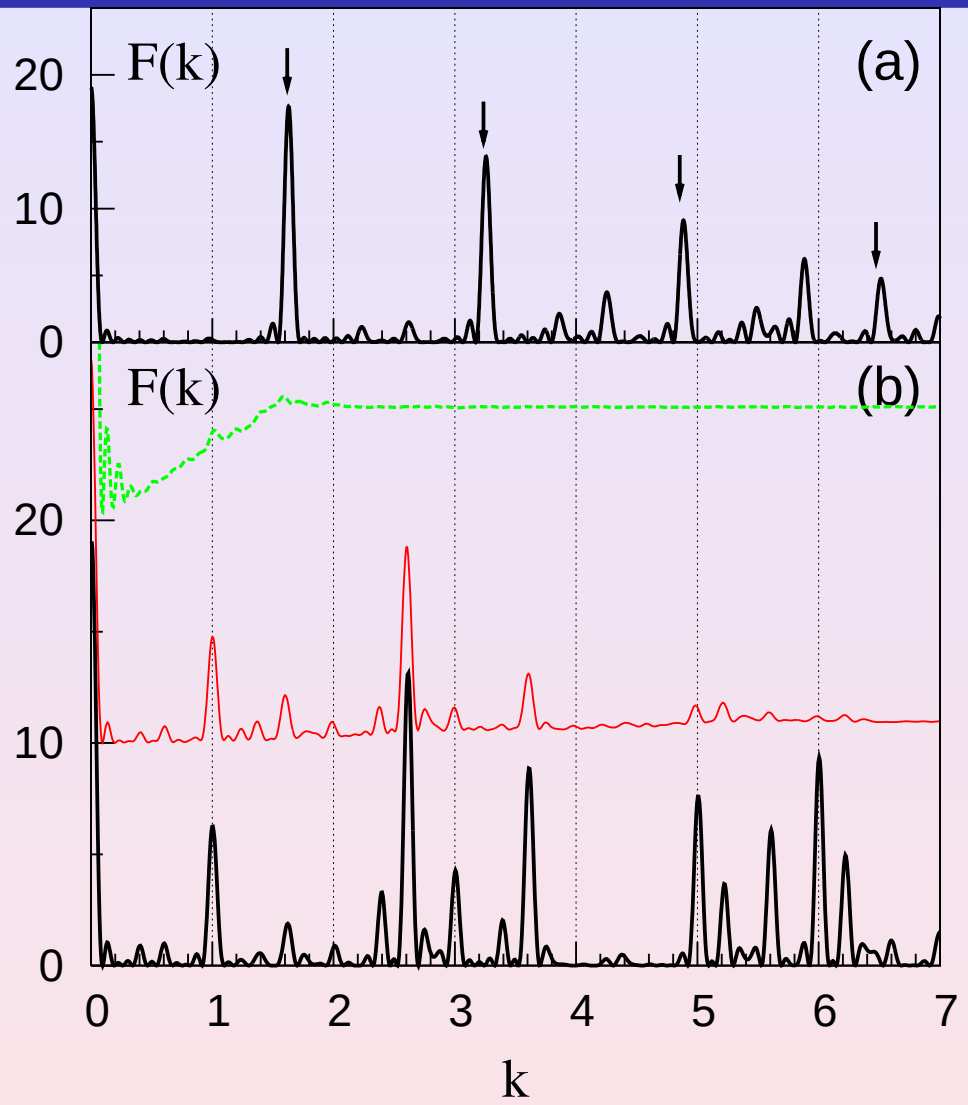

Formfactor of charge density

$F(k) =< |\sum_j \exp(ikx_j(\tau))|^2 >$

(a) The classical incommensurate phase at $K = 0.03$, $\hbar = 0$, arrows mark the peaks at integer multiples of golden mean density ν_g. (b) The pinned phase case at $K = 0.2$ for $\hbar = 0$ (bottom black curve), $\hbar = 0.1$ (red curve shifted 10 units upward), $\hbar = 2$ (green curve shifted 20 units upward, for clarity $F(k)$ is multiplied by factor 5); temperature is $T = \hbar/400 \ll K$. The quantum phase transition takes place at $\hbar_c \approx 1$.

$\rightarrow$ **SLIDING at $\nu_{c1} < \nu$, PINNING at $\nu < \nu_{c1}$**

Thermoelectricity of Wigner crystal in a periodic potential

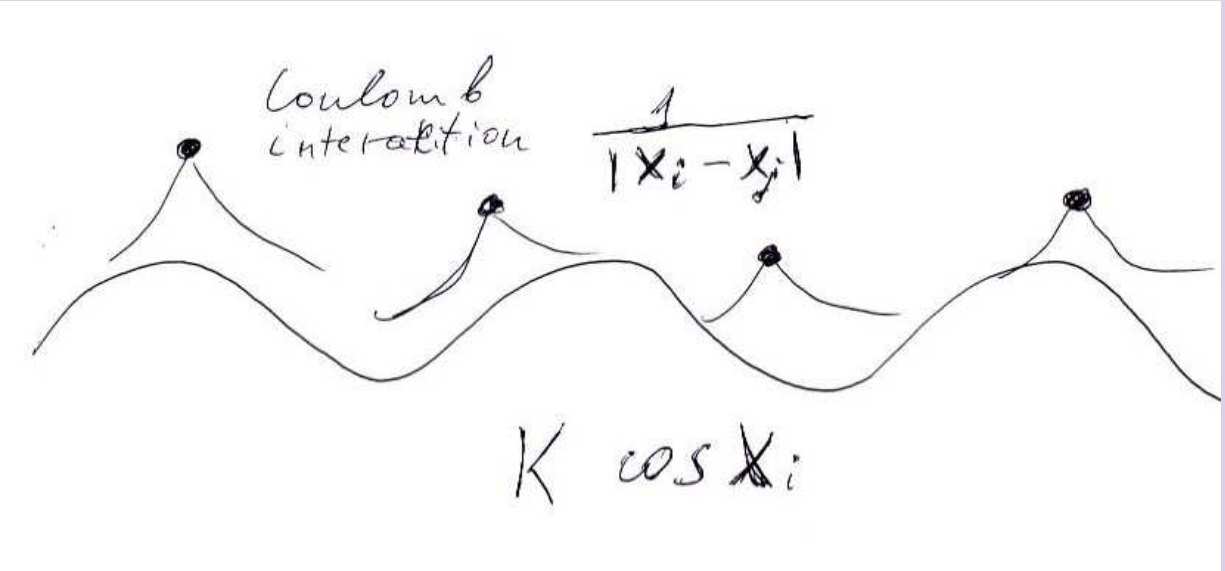

Hamiltonian $H = \sum_i \left(\frac{p_i^2}{2} + K \cos x_i + \frac{1}{2} \sum_{j \neq i} \frac{1}{|x_i - x_j|} \right)$

Dynamic equations $\dot{p}_i = -\partial H / \partial x_i + E_{dc} - \eta p_i + g \xi_i(t)$, $\dot{x}_i = p_i$

Here the Langevin force is given by $g = \sqrt{2\eta T}$, $\langle \xi_i(t) \xi_j(t') \rangle = \delta_{ij} \delta(t - t')$;
$n_e = \nu / 2\pi$, $\nu = \nu_g = 1.618...$ Fibonacci rational approximates.

Aubry transition at $K = K_c = 0.0462$ => KAM theory + chaos
I.Garcia-Mata, O.Zhirov, DLS EPJD **41**, 325 (2007)

Seebeck coefficient

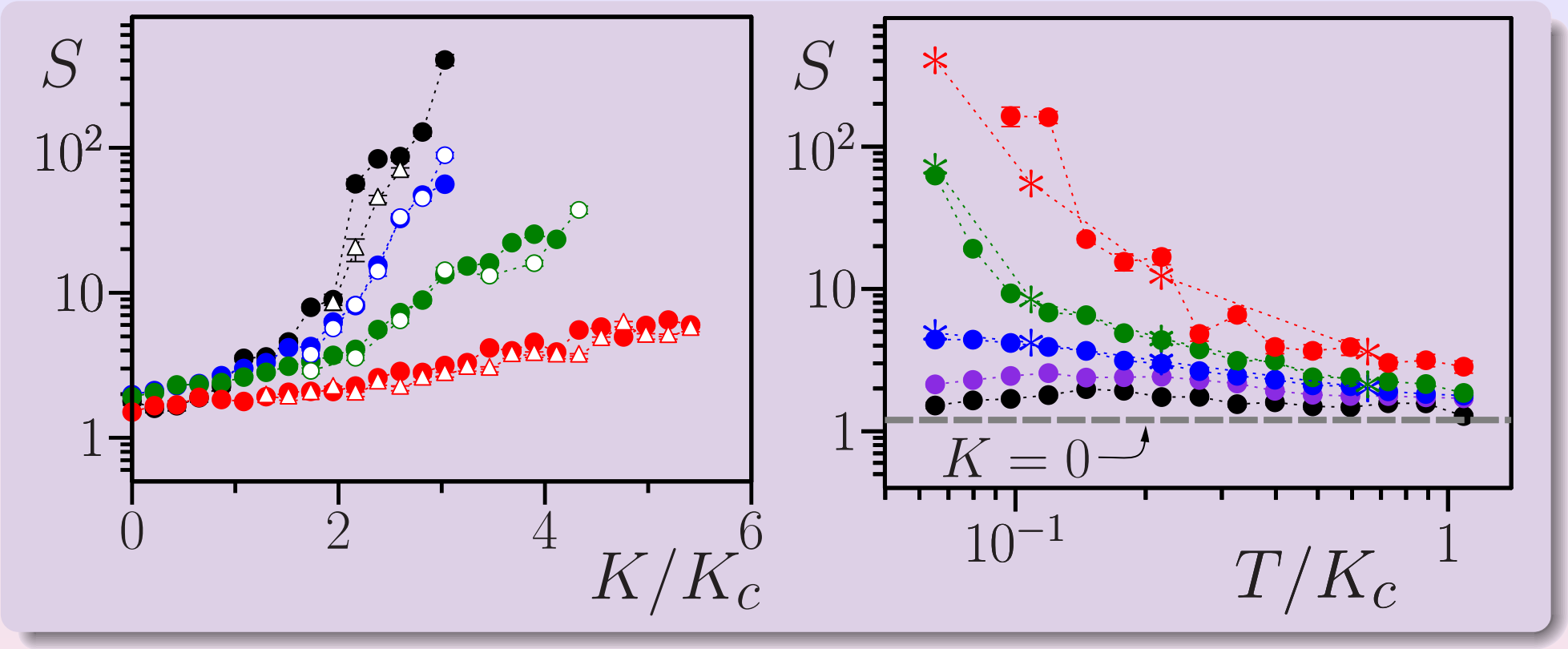

Left panel: Dependence of the Seebeck coefficient S on rescaled potential amplitude K/K_c at temperatures $T/K_c = 0.065, 0.11, 0.22$ and 0.65 shown by black, blue, green and red colors, respectively from top to bottom. The full and open symbols correspond respectively to chains with $N = 34$, $M = 21$ and $N = 55$, $M = 34$. *Right panel*: Dependence of S on T/K_c at different $K/K_c = 0, 0.75, 1.5, 2.2, 3$ shown respectively by black, violet, blue, green and red points; $N = 34$, $M = 21$; the dashed gray line shows the case $K = 0$ for noninteracting particles. The stars show corresponding results from left plane at same N, M. Dotted curves are drown to adapt an eye. Here and in other Figs. the statistical error bars are shown when they are larger than the symbol size. Here $\eta = 0.02$.

Conductivity and thermal conductivity

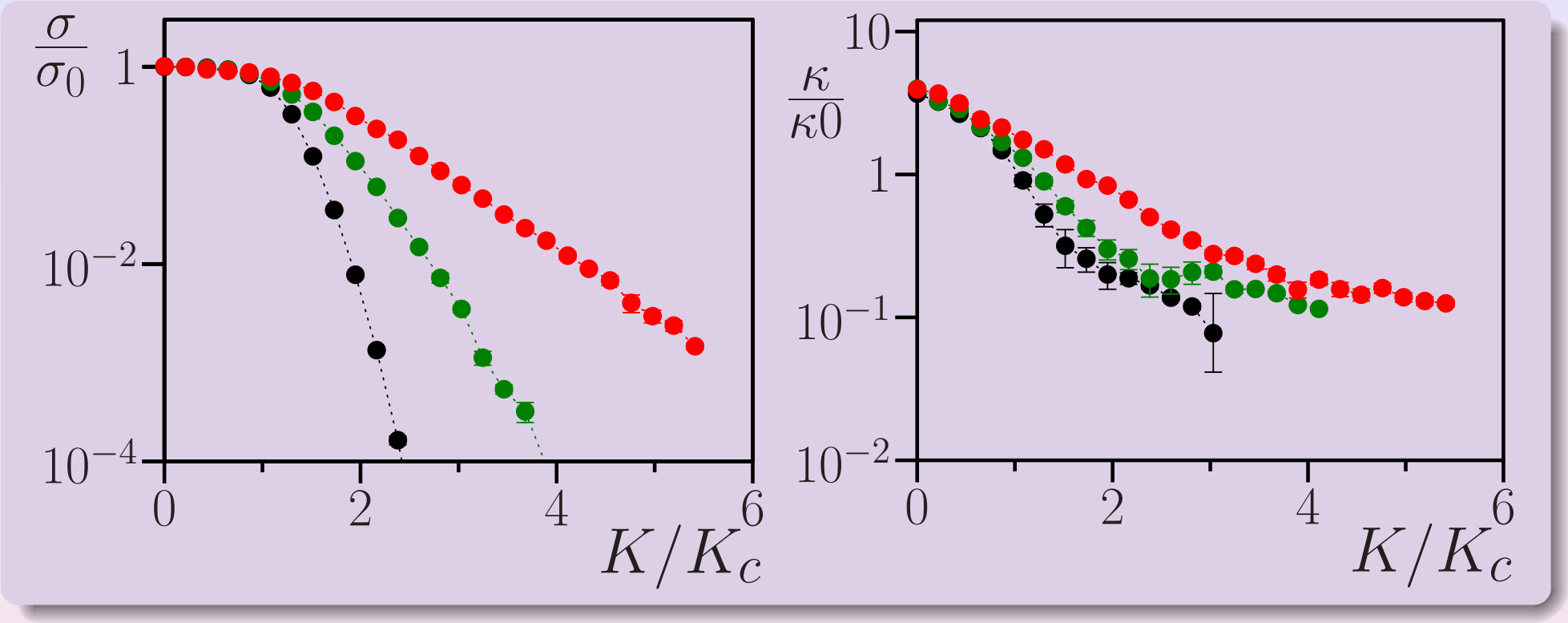

Left panel: Rescaled electron conductivity σ/σ_0 as a function of K/K_c shown at rescaled temperatures $T/K_c = 0.065$, 0.22, 0.65 by black, green and red points respectively. *Right panel*: Rescaled thermal conductivity κ/κ_0 as a function of K/K_c shown at same temperatures and colors as in left panel. Here we have $N = 34$, $M = 21$, $\eta = 0.02$, $\sigma_0 = \nu_g/(2\pi\eta)$, $\kappa_0 = \sigma_0 K_c$.

ZT dependence on parameters $\nu \approx 1.618$

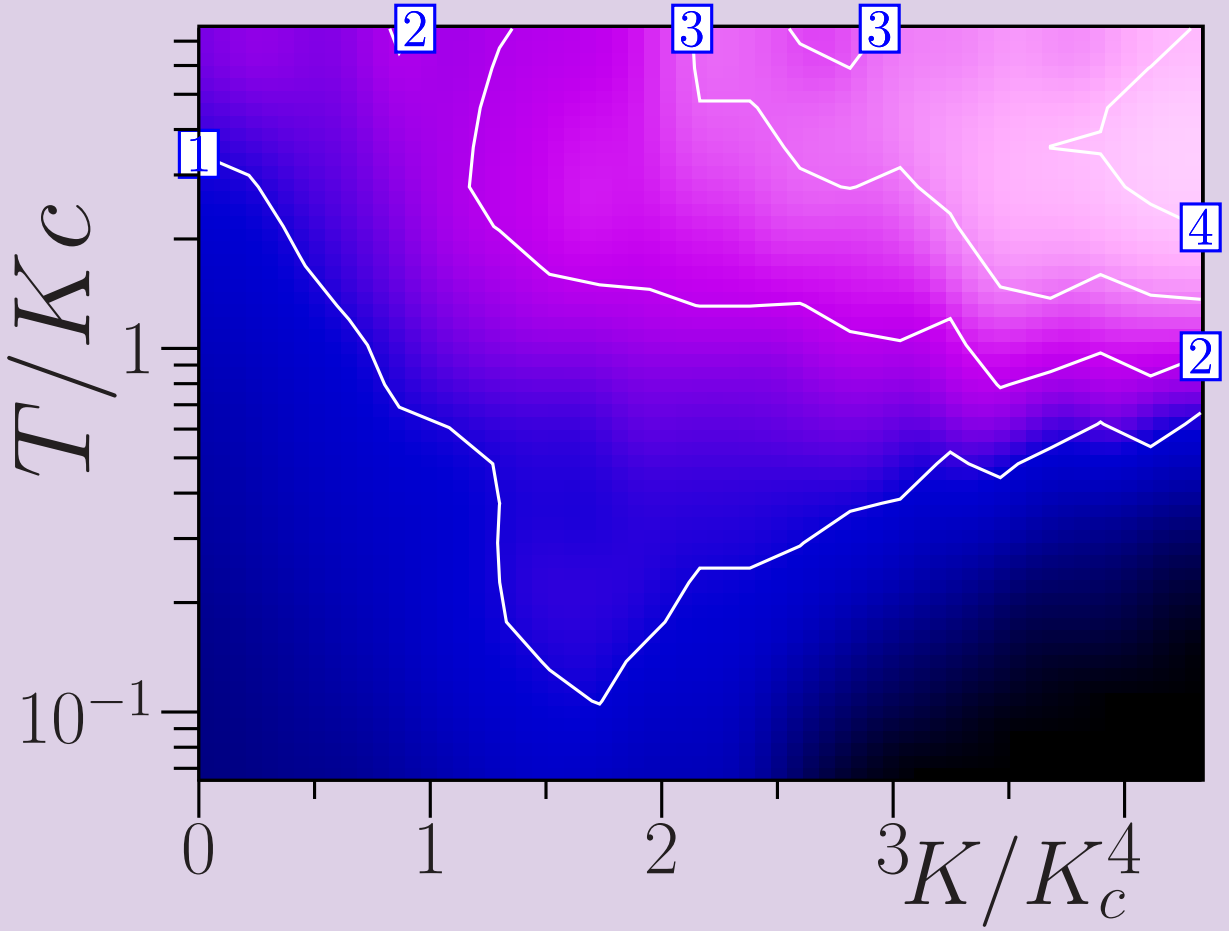

Dependence of ZT on K/K_c and T/K_c shown by color changing from $ZT = 0$ (black) to maximal $ZT = 4.5$ (light rose); contour curves show values $ZT = 1, 2, 3, 4$. Here $\eta = 0.02$, $N = 34$, $M = 21$.

ZT dependence on parameters $\nu \approx 0.618$

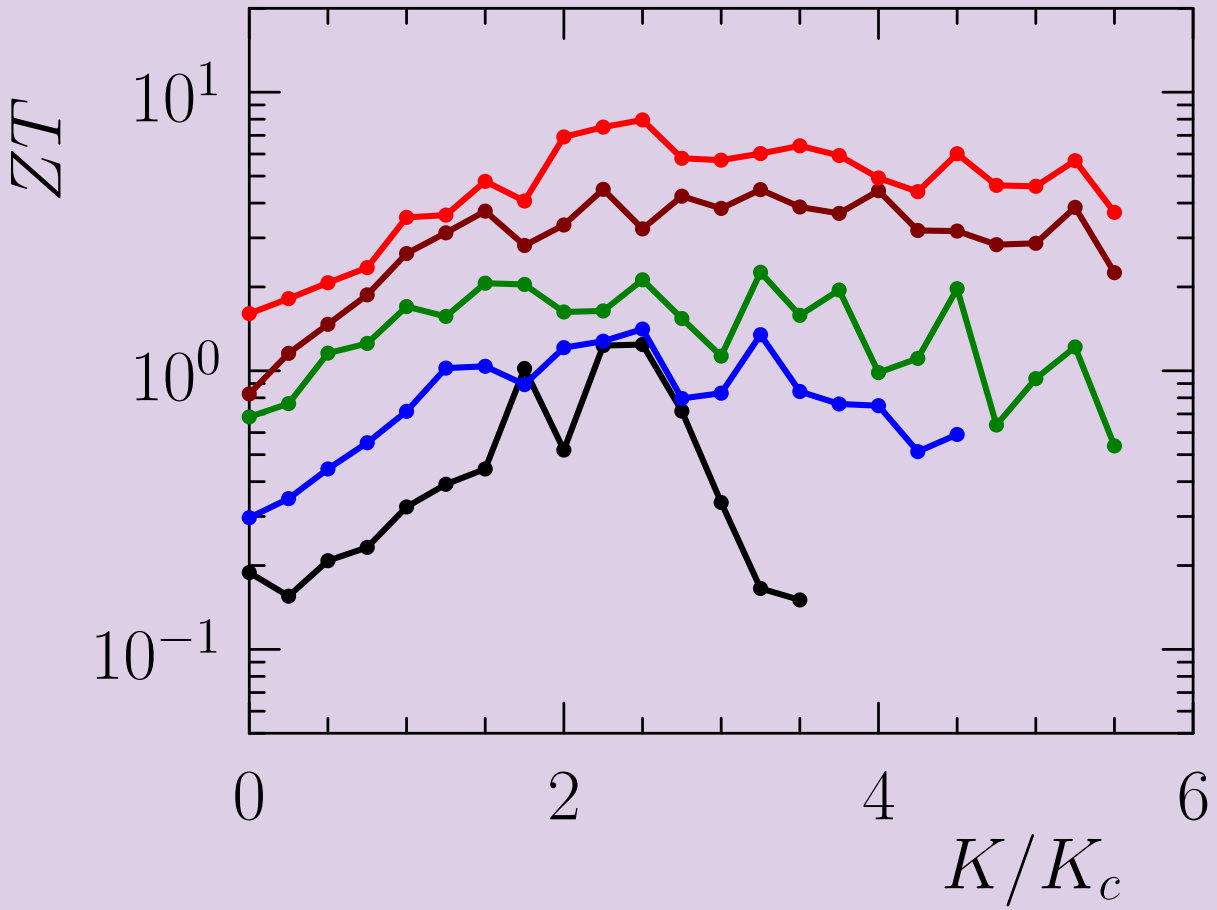

Dependence of ZT on K/K_c at different temperatures $T/K_c = 0.25$ (black), 0.5 (blue), 1 (green), 1.5 (brown), 2 (red). Here there are $N = 21$ ions in $L = 34$ periods with $N/L \approx \nu \approx 0.618..$ in the center; $K_c = 0.002$.

Wigner crystal diode in 2D

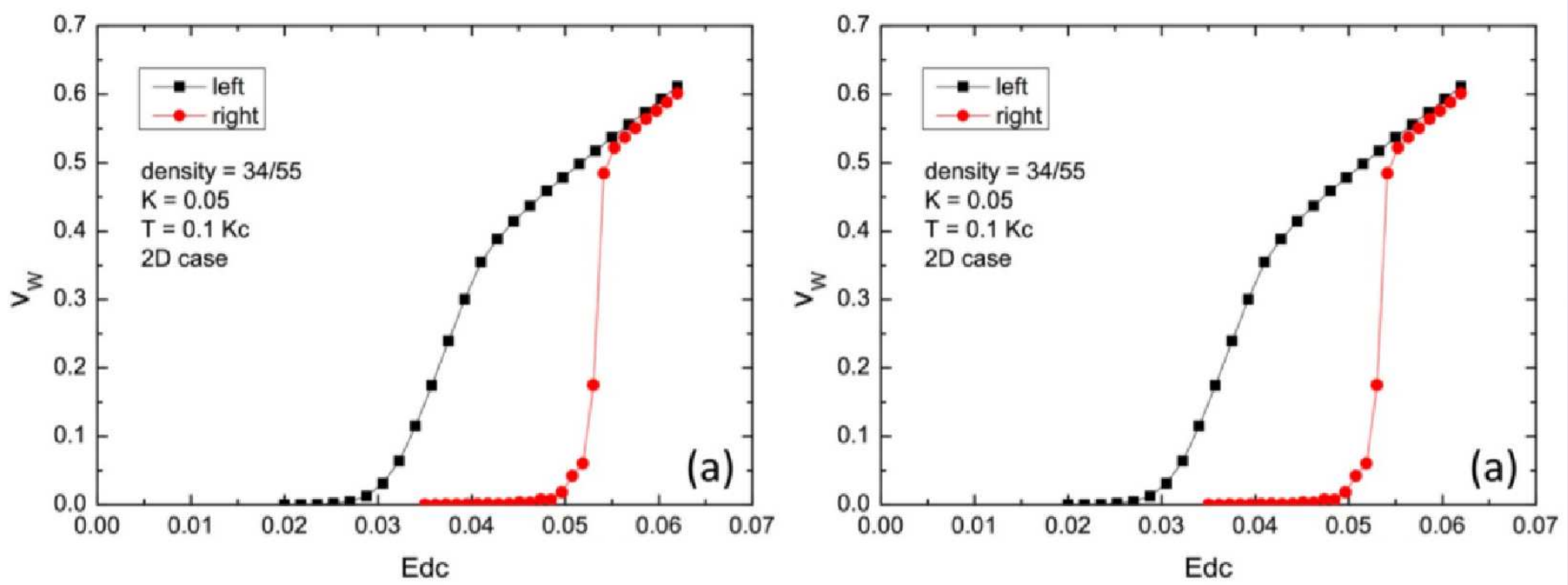

Left: 1D potential profile in 2D $V = K(\sin x + 0.4 \sin 2x - \cos y)$;
Right: Wigner crystal velocity v_W in dc-field E_{dc}
$\nu = N/L = 34/55$ (5 stripes in y)

Wigner crystal diode in 2D

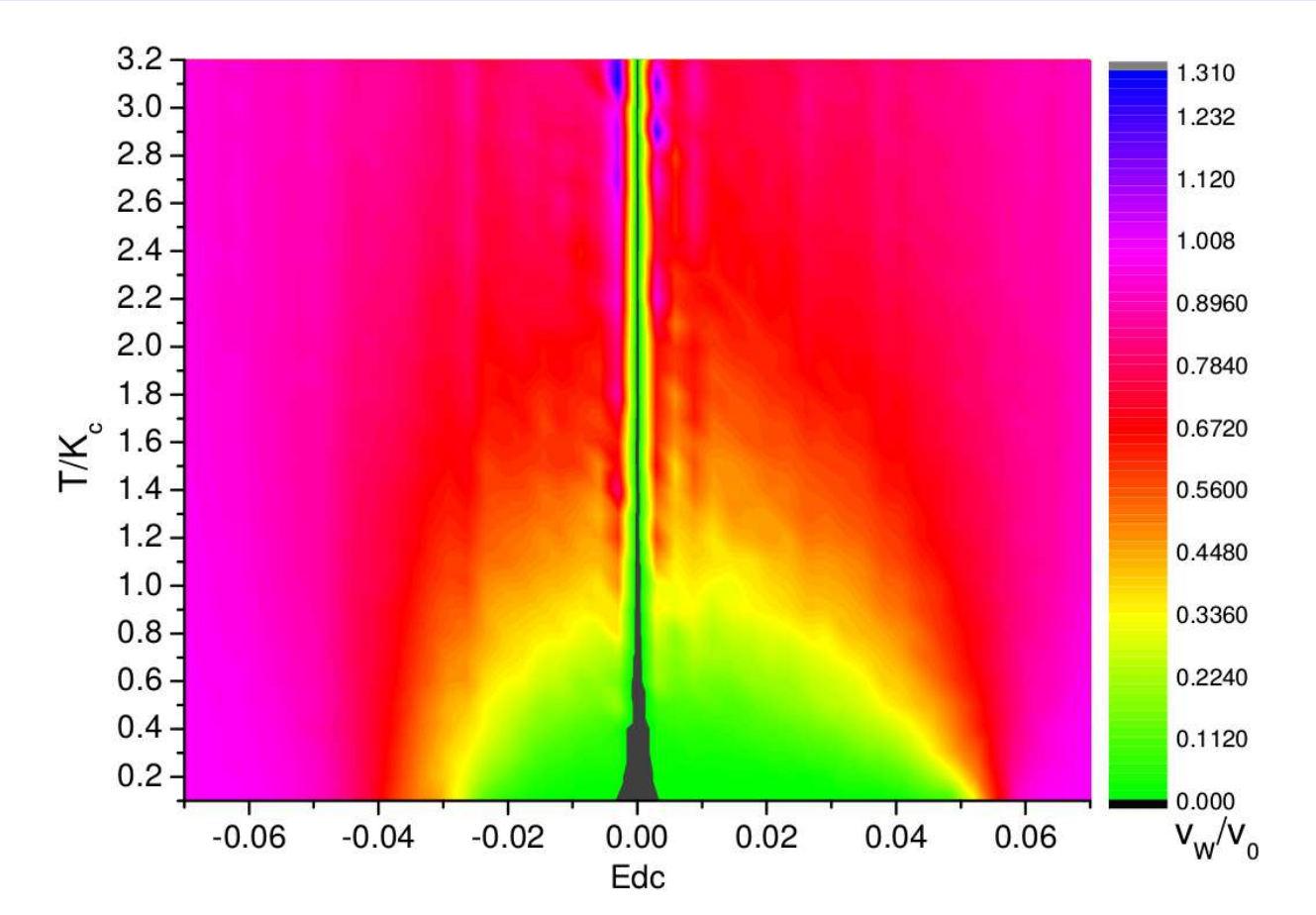

Color: rescaled Wigner crystal velocity v_W/v_0 at different *dc*-field E_{dc} and rescaled temperature T/K_c; $K_c = 0.0462$, $\eta = 0.1$, $v_0 = E_{dc}/\eta$; $\nu = N/L = 34/21$ (5 stripes in y)

Zakharov, Demidov, DS PRB (2019)

Ion quantum computers

Cirac-Zoller 1995 proposal; experiments Wineland, Blatt et al 1995-2008; Haroche-Wineland Nobel prize 2012 for ground-breaking experimental methods that enable measuring and manipulation of individual quantum systems: oscillator global trap, a few micron ion distance, individual ion access by laser; two-qubit gate by laser pulses and recoil transfer between ions

2018: 100 ions routinely kept for hours (Monroe U Maryland arXiv2018)

Cryogenic Trapped-Ion System for Large Scale Quantum Simulation 9

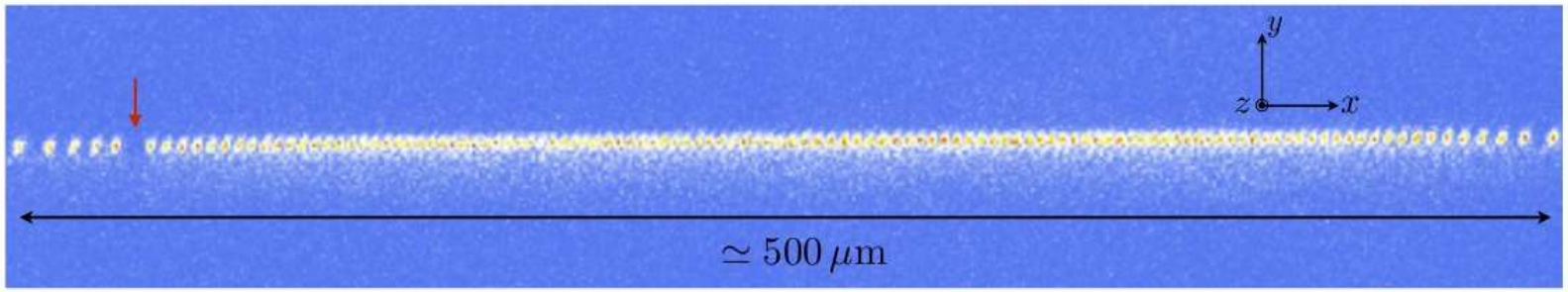

Figure 5. Linear chain of 121 $^{171}Yb^{+}$ ions. In this case $\omega_y/2\pi = 1.5$ MHz and $\omega_x/2\pi = 35$ kHz. The axial confinement has been relaxed to resolve all the center ions

From 2019: 5 arXiv-Nature-Science preprint/articles (IonQ-Maryland-Innsbruck) on quantum computing with up to 11 qubits; best gate fidelity is 99.9999% (1-qubit), 99.9% (2-qubit)

Problem of Large scale quantum computers:
Cirac-Zoller 1995 scheme is NOT scalable

Gap dependence on number of ions

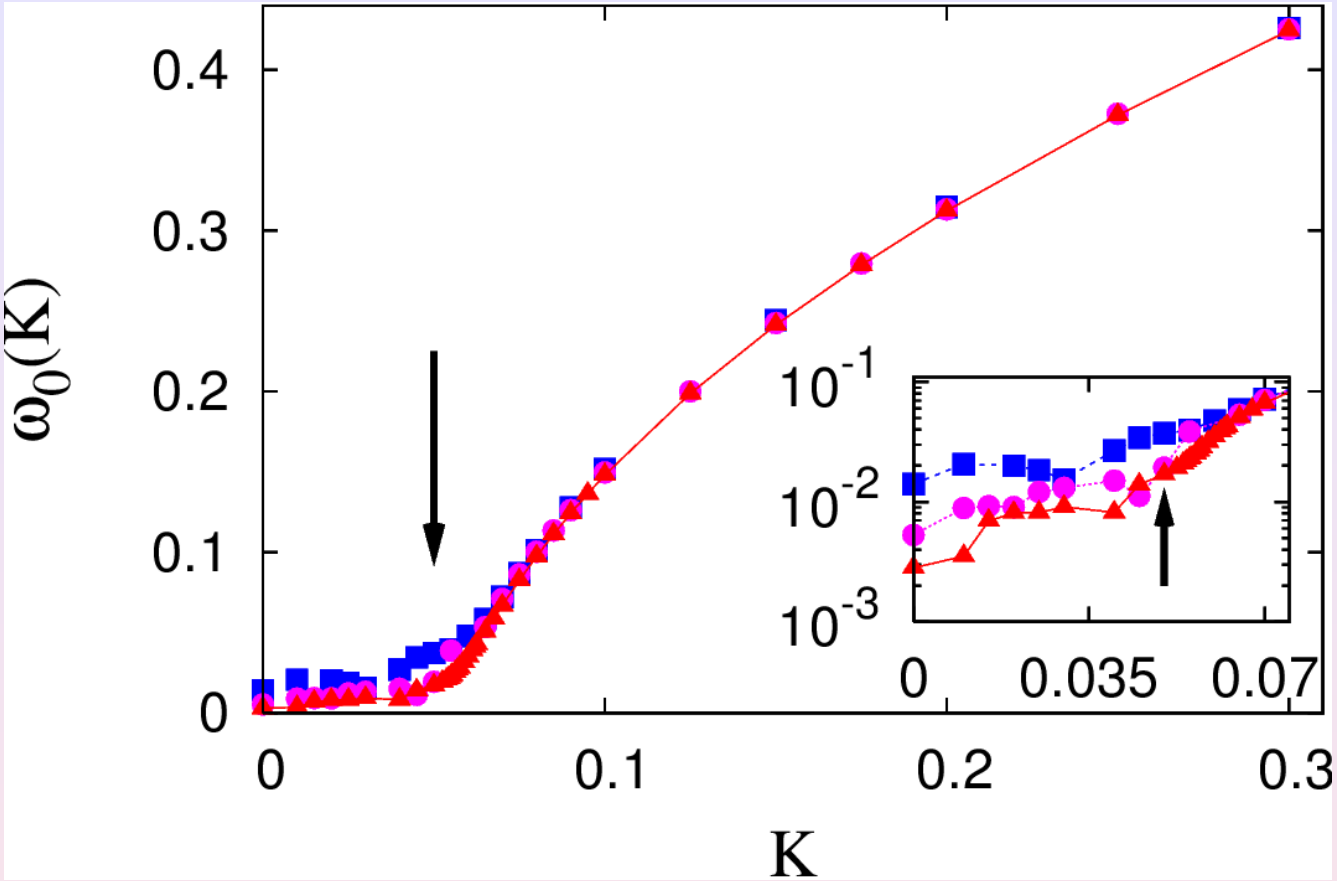

Minimal phonon excitation frequency $\omega_0(K)$ as a function of potential stength K for the golden mean density $\nu = \nu_g = 1.618...$ and number of ions $N = 50$ (blue squares, $\omega_{tr} = 0.014$); $N = 150$ (magenta circles, $\omega_{tr} = 0.00528$); $N = 300$ (red triangles, $\omega_{tr} = 0.00281$); the critical point of Aubry transition at $K \approx 0.05$ is marked by arrow; inset shows data near K_c.

DS arXiv (2019), DS et al. EPJD (2007)

Experiments for Aubry transition, quantum gates, phonon modes

* Experiments:
Vuletic group (MIT) (Nature Mat. (2016) 5 ions)
Mehlstaubler group (PTB DE, Nature Comm. (2017))
Drewsen group (Aarhuss U DK PRA (2019)
Paul trap 8 ions)

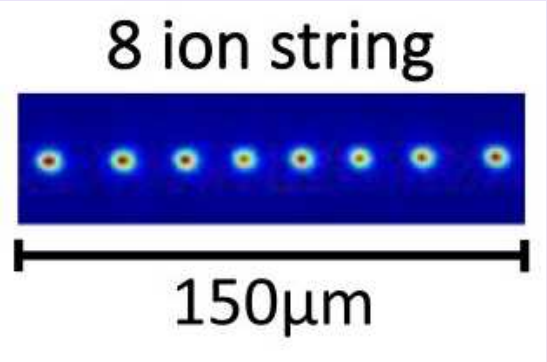

* Quantum gates are performed by laser pulses assuming harmonic motion of ions; in reality we have a quantum many-body interacting systems and numerical modeling of gates should take into account properties of quantum low energy excitations $\rightarrow$ advanced methods of quantum chemistry

* Towards analysis of low energy phonon modes and modeling the accuracy of quantum gates with numerical simulations
(Aubry-Andre localization; Anderson localization)

* Experimental progress with microtrap arrays (about 30 micron spacing)

Physical picture in oil ...

* - Experimental observation of Aubry transition with cold ions in a periodic optical lattice by Vuletic group (MIT) Nat. Mat. **11**, 717 (2016)

* - A lot of numerical computations for different materials
(e.g. Kozinsky et al. (Bosch-Harvard) Jour. Appl. Phys. **119** 205102 (2016))
BUT ELECTRON-ELECTRON INTERACTIONS
ARE NOT TREATED CORRECTLY
=> NEW CHALLENGE FOR MATERIAL-COMPUTER SCIENCE

* - Interacting electrons in presence of incommensurate density ?

* - Aubry pinned phase with electrons on liquid helium
(Rees, Yeh, Lee, Kono, Lin PRB **96**, 205438 (2017);
Lin, Smorodin, Badrutdinov, Konstantinov J.Low.Temp.Phys. (2018))

* - Quantum computer with electrons on liquid helium in the Aubry phase
(extending proposal of Platzman, Dykman Science (1999))

* - TWO POSSIBLY USEFUL POINTS OF AUBRY PHASE:
THERMOELECTRICITY AND QUANTUM COMPUTING